HHS Public Access
Author manuscript
J Chem Inf Model. Author manuscript; available in PMC 2024 September 25.

Published in final edited form as:
J Chem Inf Model. 2023 September 25; 63(18): 5896–5902. doi:10.1021/acs.jcim.3c00227.

Deciphering the Allosteric Activation Mechanism of SIRT6 using Molecular Dynamics Simulations

Zhiyuan Zhao[a,#], **Jintong Du**[a,b,#], **Yu Du**[a], **Yuan Gao**[a], **Mingxuan Yu**[a], **Yingkai Zhang**[c,d], **Hao Fang**[a], **Xuben Hou**[a]

[a]Department of Medicinal Chemistry and Key Laboratory of Chemical Biology of Natural Products (MOE), School of Pharmaceutical Science, Cheeloo College of Medicine, Shandong University, Jinan, Shandong 250012, China

[b]Shandong Cancer Hospital and Institute, Shandong First Medical University, Jinan, Shandong 250117, China

[c]Department of Chemistry, New York University, New York, NY 10003, United States

[d]Simons Center for Computational Physical Chemistry at New York University, New York, NY 10003, United States

Abstract

As a member of the histone deacetylase protein family, the NAD^+-dependent SIRT6 plays an important role in maintaining genomic stability and regulating cell metabolism. Interestingly, SIRT6 has been found to have a preference for hydrolyzing long-chain fatty acyls relative to deacetylation, and it can be activated by fatty acids. However, the mechanisms by which SIRT6 recognizes different substrates and can be activated by small molecular activators are still not well understood. In this study, we carried out extensive molecular dynamic simulations to shed light on these mechanisms. Our results revealed that the binding of the myristoylated substrate stabilizes the catalytically favorable conformation of NAD^+, while the binding of the acetyl-lysine

Corresponding authors Xuben Hou-Department of Medicinal Chemistry and Key Laboratory of Chemical Biology of Natural Products (MOE), School of Pharmaceutical Science, Cheeloo College of Medicine, Shandong University, Jinan, Shandong 250012, China; hxb@sdu.edu.cn; **Hao Fang**-Department of Medicinal Chemistry and Key Laboratory of Chemical Biology of Natural Products (MOE), School of Pharmaceutical Science, Cheeloo College of Medicine, Shandong University, Jinan, Shandong 250012, China; haofangcn@sdu.edu.cn**; Yingkai Zhang**-Department of Chemistry, New York University, New York, NY 10003, United States; Simons Center for Computational Physical Chemistry at New York University, New York, NY 10003, United States; yingkai.zhang@nyu.edu.
Zhiyuan Zhao-Department of Medicinal Chemistry and Key Laboratory of Chemical Biology of Natural Products (MOE), School of Pharmaceutical Science, Cheeloo College of Medicine, Shandong University, Jinan, Shandong 250012, China
Jintong Du-Department of Medicinal Chemistry and Key Laboratory of Chemical Biology of Natural Products (MOE), School of Pharmaceutical Science, Cheeloo College of Medicine, Shandong University, Jinan, Shandong 250012, China; Shandong Cancer Hospital and Institute, Shandong First Medical University, Jinan, Shandong 250117, China
Yu Du-Department of Medicinal Chemistry and Key Laboratory of Chemical Biology of Natural Products (MOE), School of Pharmaceutical Science, Cheeloo College of Medicine, Shandong University, Jinan, Shandong 250012, China
Yuan Gao -Department of Medicinal Chemistry and Key Laboratory of Chemical Biology of Natural Products (MOE), School of Pharmaceutical Science, Cheeloo College of Medicine, Shandong University, Jinan, Shandong 250012, China
Mingxuan Yu-Department of Medicinal Chemistry and Key Laboratory of Chemical Biology of Natural Products (MOE), School of Pharmaceutical Science, Cheeloo College of Medicine, Shandong University, Jinan, Shandong 250012, China
Author contributions
Z.Z. and J.D. contributed equally to this work

Supporting Information
Supplementary Figure S1-S2 (PDF). This material is available free of charge via the Internet at http://pubs.acs.org.

The authors declare no competing financial interest.

substrate leads to a loose binding of NAD^+ in SIRT6. Based on these observations, we proposed a reasonable allosteric binding mode for myristic acid, which can enhance the catalytic activity of SIRT6 by stabilizing the binding of NAD^+ with His131 as well as the acetylated substrate. Furthermore, our molecular dynamics simulations demonstrated that synthetic SIRT6 activators, such as UBCS039, MDL-801, and 12q, block the flipping of ribose in NAD^+ and therefore can stabilize substrate-NAD^+-His131 interactions in a manner similar to fatty acids. In summary, our newly proposed activation mechanism of SIRT6 highlights the importance of protein-substrate interactions, which would facilitate the rational design of new SIRT6 activators.

Graphical Abstract:

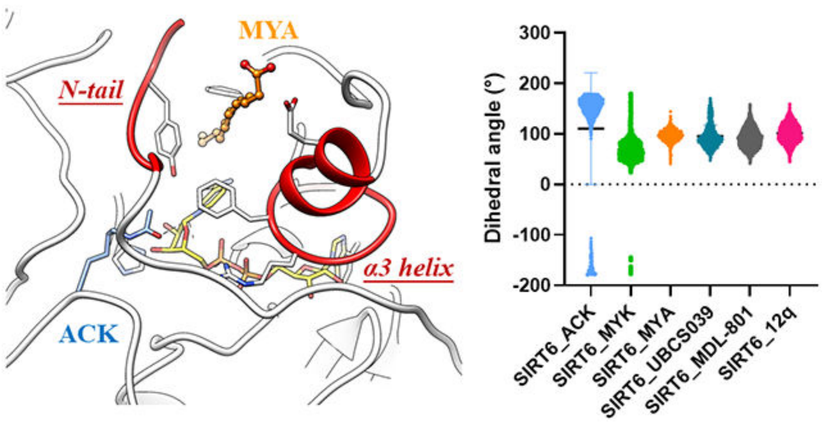

Keywords

Enzyme Activation; SIRT6; Protein-Substrate Interaction; Molecular Dynamics Simulation

Introduction

The Sirtuin protein family consists of seven members (SIRT1-SIRT7), serving as NAD^+-dependent lysine deacetylases and located at different subcellular locations.[1] Sirtuins play a crucial role in many physiological processes such as regulating lifespan extension and controlling various metabolic pathways.[2, 3] As an important member of Sirtuins, SIRT6 extensively participates in the deacetylation of histones (e.g. H3[4, 5]) and non-histones, which are closely associated with DNA damage repair, maintenance of telomere integrity, transcriptional regulation, and cellular energy metabolism.[6-9]

In particular, SIRT6 has been shown to function as a tumor suppressor gene, therefore, the development of SIRT6 activators has gained many research interests.[10, 11] Interestingly, previous research showed that SIRT6 prefers to hydrolyze long-chain fatty acyl groups rather than acetyl groups.[12] Furthermore, endogenous long-chain fatty acids (e.g. myristic acid, lysophosphatidic acid) have been found to increase the deacetylase activity of SIRT6.[13] In recent years, several small molecular activators have also been reported, including UBCS039[14], MDL-801[15], and 12q[16] (Figure 1B). Recently, Lu et al. reported that rotation of the R-ring conformation of MDL-801 is an important contribution to SIRT6 activation.[17] Especially, these molecules activate SIRT6 allosterically and showed high selectivity against other sirtuins. Recently, several natural products and an approved drug (Fluvastatin) have been found to be SIRT6 allosteric activators.[18, 19] Nowadays, activation of SIRT6 has been proven to be beneficial for the treatment of cancer.[20]

Heretofore, the detailed mechanisms for substrate recognition and activation of SIRT6 remain unclear. The Sirtuin family shares a conserved catalytic domain but is different in the N-terminal and C-terminal domains.[21-23] Compared to other Sirtuins members, SIRT6 consists of a small splayed zinc-binding motif domain and a large Rossmann fold domain which bind NAD^+ and substrate (Figure 1 A).[12, 24] Especially, SIRT6 lacks a helix bundle that concatenates the zinc-binding domain and Rossmann fold domain as well as the conserved-existing NAD^+-binding loop existing in other Sirtuins (Figure S1 in Supporting Information). Hence, this structural difference may be related to the experimental observation that SIRT6-dependent histone deacetylation is about one thousand-fold slower than the other SIRT member.[24] The mechanism for the deacetylation reaction of sirtuins was described in Figure 1 C: the first stage involves the nucleophilic attack and the removal of the nicotinamide. After that, the second stage is more complex and includes a rate-determined step according to previous research.[25] Especially, residue His131 acts as a crucial residue to transfer proton in this process highlighting the importance of substrate-protein interaction in SIRT6 deacetylation reaction.

Molecular dynamics (MD) simulations have been successfully employed in the investigation of catalytic or inhibition mechanisms of sirtuins.[25-28] In the current study, we performed extensive MD simulations using SIRT6-substrate complexes with or without activator-bound to explore the detailed activation mechanism. Our results not only explained previous experimental observations that SIRT6 exhibited superior defatty-acylation to deacetylation, but also proposed a general mechanism for SIRT6 small molecular activators. Our study provided a new starting point for the future design of SIRT6 activators.

Results and Discussion

Long-chain fatty substrate stabilize the catalytic favorable conformation of NAD^+.

To further clarify the preference of SIRT6 against different substrates, we performed molecular dynamics (MD) simulations using SIRT6-myristoylated substrate complex (SIRT6-MYK) and SIRT6-acetyl lysine substrate complex (SIRT6-ACK) with or without activator bound (Table 1). Based on the catalytic mechanism for sirtuin-catalyzed deacetylation reactions (Figure 1C), the first step of the reaction is the transfer of the acetyl group attached to the substrate lysine residue to the NAD^+, yielding nicotinamide and other intermediates. Thus, the spatial position of NAD^+ relative to acetylated lysine is critical. Herein, we have mainly compared the distance between ACK/MYK@O and NAD^+@C as well as the angle at which ACK/MYK@O attacks NAD^+@C in each MD system. Compared to the SIRT6-myristoylated substrate complex, there was a large unfilled hydrophobic pocket in SIRT6-acetylated substrate complexes (Figure 2A-B). This packing defect led to the “flipping out” of the ribose ring of NAD^+ during MD simulation, while the long-chain fatty substrate stabilized a proper configuration of NAD^+. The distance between ACK@O and NAD^+@C in the SIRT6-MYK system (4.63±0.85 Å) was closer than the SIRT6-ACK system (6.19±0.87 Å) and the calculated energy barrier for the first catalytic step in SIRT6-MYK system was significantly lower than that of SIRT6-ACK system (Figure 2D-E). Additionally, in the SIRT6-MYK system, MYK@O attacks NAD^+ at a more appropriate angle, while in the SIRT6-ACK system, a higher spatial site resistance to the catalytic reaction occurs due to the flip of the NAD^+ conformation (Figure 2F), where Phe62 may play an important role. In the SIRT6-MYK system, Phe62 was flipped and its benzene ring is restricted to a relatively fixed conformation, which favored the maintenance of a relatively catalytically favorable conformation of NAD^+ (Figure 2C). We also observed the dissociation of His131 and NAD^+ in the SIRT6-ACK system, implying that this packing defect may also affect the second stage of sirtuin-catalyzed deacetylation (Figure 1C). Therefore, our computational results suggested that the unoccupied hydrophobic channel led to the loose binding of NAD^+, while long-chain fatty substrates could well occupy this pocket and stabilize the binding of the NAD^+-SIRT6 complex. The above results explained the experimentally observed preference of SIRT6 against the fatty acylated substrate and provided important clues to investigate the activation mechanism of SIRT6.

Myristic acid compensates the packing defect of the SIRT6 catalytic site.

As previously reported, the deacetylation activity of SIRT6 could be augmented by endogenous fatty acids, however, the detailed activation mechanism remains unclear. Inspired by the computational results, we speculated that the activation mechanism of endogenous fatty acids may also depend on the stabilization of NAD^+-acetylated substrate interactions. Previous research has suggested that fatty acid may bind to the same hydrophobic channel with myristoylated peptide[13]. Therefore, we initially speculated that myristic acid could bind to the unoccupied substrate binding channel in the SIRT6-ACK complex (Figure 2B). Using the molecular docking strategy, we constructed two representative binding poeses (MYA-I and MYA-II) of myristic acid with opposite insert directions (Figure 3A). To further evaluate the binding mode of myristic acid, we performed MD simulations for each system and analyzed the impacts of fatty acid on SIRT6.

As shown in Figure S2 in Supporting Information, both MYA-I and MYA-II become stable after 200ns of MD simulation. Interestingly, the binding of MYA-I stabilized the substrate-NAD^+ interaction, in a similar manner with the SIRT6-MYK system. As shown in Figure 3B, the distance between ACK@O and NAD^+@C in the SIRT6-MYA-I system (5.22±0.68Å) was significantly closer than the SIRT6-ACK system (6.19±0.87Å) and the SIRT6-MYA-II system(6.07±1.17Å). To explore the detailed activation mechanism of myristic acid, we also compared the dihedral angle that determined the conformation of NAD^+ for catalysis and found that the dihedral angle distribution of the MYA-I group was mainly distributed at 96.87±11.42°, showing the effect of the myristic acid in stabilizing interaction between substrate and NAD^+ (Figure S3 in Supporting Information). We further calculated and compared the free energy of the two docking postures in the first step of the catalytic deacetylation reaction and found that the reaction free energy barrier of the docking pose I decreased to 1.57 kcal/mol, which was lower than that of the docking pose II with a reaction free energy barrier of 5.13 kcal/mol (Figure 3C). Therefore, we proposed an activation mechanism for long-chain fatty acid activators: the binding of myristic acid compensating the packing defect of key catalytic site and stabilizing the interaction of NAD^+

with the substrate acetyl group. Furthermore, the presence of myristic acid enabled the acetyl group on the substrate to attack NAD^+ in an appropriate dihedral that facilitates the nucleophilic substitution reaction.

Compared to the initial docking result, myristic acid (MYA-I system) rotates approximately 90 degrees from the initial pocket, moves out of the hydrophobic channel, finally anchored stably in the α3 helix and its terminal group was close to the nicotinamide of NAD^+, compensating for the packing defect of the key catalytic site (Figure 3A and 3D). According to the predicted binding mode, myristic acid extensively formed stable hydrophobic interactions with surrounding residues including Tyr3, Ile59, Pro60, Pro78, Leu76, Val113 and formed a hydrogen bond interaction with Gly75, reflecting the key role of hydrophobic interactions in stabilizing the binding mode of myristic acid (Figure S4 in Supporting information). In particular, we found that the predicted binding site of myristic acid overlapped with the pocket that accommodates the synthetic activators (e.g. UBCS039 and MDL-801) (Figure 4A), further highlighting the versatility of this allosteric pocket in SIRT6 activation.

The synthetic allosteric activator universally blocks the flipping of ribose in NAD^+.

UBCS039 is the first reported synthetic SIRT6 activator.[14] Subsequently, several more potent SIRT6 activators (e.g. MDL-801, 12q) have been developed.[15, 16] The co-crystal structures of UBCS039 and MDL-801 with SIRT6 have also been determined, providing good starting points for our investigation.[14, 15] Additionally, the predicted 12q binding pocket is similar to that of MDL-801 and UBCS039, indicating that synthetic allosteric activators share a similar allosteric regulation pocket behind the substrate site (Figure 4A). Therefore, we further investigated whether our proposed SIRT6 activation mechanism is applicable for different activators.

Then, we performed MD simulations of SIRT6 complexed with different activators and analyzed the distances as well as dihedral angles between substrate and NAD^+, which have been proven to be highly related to SIRT6 activation (Figure 2 and Figure 3). As shown in Figure 4B, the average dihedral angle between the substrate and the cofactor of the SIRT6 activator systems (MYA: 96.87±11.42°; UBCS039: 95.59±22.33°; MDL-801: 91.71±19.30°; 12q: 101.27±18.49°) were closer to the SIRT6-MYK system (68.47±18.94°) than to the SIRT6-ACK system (110.45±110.74°). In addition, as the ribose conformation of NAD^+ is flipped in the SIRT6-ACK system, the distance of ACK@O and NAD^+@C is increased, which impaired the deacetylation reaction (Figure 4C). We further investigated the structural basis of these changes and found that when the activator binds to the allosteric pocket formed by the N-tail and α3 helix, it causes rotation of the α3 helix, which then created a suitable catalytic pocket for the acetylated substrate. During this process, the residue Phe62 is flipped, assisting the ribose in NAD^+ to adopt a conformation that favors the catalytic reaction and facilitates hydrogen bonding interactions between the ribose in NAD^+ and His131 (Figure 4D). Moreover, due to the flexibility of the N-tail, it is possible to bind different activators and stabilize the NAD^+-Substrate-SIRT6 interaction.

Computational method

Structure preparation.—For the entire SIRT6 simulation system, the crystal structure of the SIRT6-Myristoyl Lysine substrate complex (PDB code: 3ZG6) was used as the initial structure. The SIRT6-acetyl lysine substrate complex was generated by manually editing the Myristoyl lysine substrate. The conformation of co-factor NAD^+ was adopted from the SIRT1 crystal structure (PDB code: 4I5I). For activator-bound systems, the conformation of MDL-801 and UBCS039 was adopted from crystal structures (PDB code: 7CL1 and 5MF6). The 12q conformation was adopted from previous docking research.[16] Myristic acid was docked into the hydrophobic channel between the zinc binding motif domain and the Rossmann fold domain by AutoDock Vina. Two typical docking poses (docking pose I and II) for myristic acid were chosen according to the direction of insertion of the fatty acid chains. The protonation state of the charged residues was calculated by the PDB2PQR server based on pKa.[29, 30]

Molecular Dynamics Simulation.—All molecular dynamics simulations were performed using Amber14 molecular dynamics software. The ff14SB force field was used for proteins, and the TIP3P model was used for water molecules. Zinc parameters were developed by Zinc Amber Force Field (ZAFF).[31] The force field parameters of NAD^+ are obtained from the literature.[32] The partial charge of myristoyl-lysine substrate, acetyl-lysine substrate and small molecular activators (myristic acid, MDL-801, UBCS039 and 12q) were calculated using the AM1-BCC method. Each system was neutralized with Cl^- counterions and solvated in a rectangular periodic box with a 12.0 Å buffer using the TLEAP module in AmberTools14 with explicit TIP3P water. The particle grid Ewald method for nonbonded interactions (12.0 Å cutoff) is used for energy minimization and MD simulation. After a series of minimization and balancing, standard molecular dynamics simulations were performed on the GPU using the CUDA version of PMEMD (Particle Mesh Ewald Molecular Dynamics). For each system, two independent simulations were carried out (a total of 2 μs) with periodic boundary conditions. The SHAKE algorithm is used to constrain all the bonds involving hydrogen atoms. A time step of 2 fs was used, and the system temperature was controlled at 300K using the Berendsen thermostat method.

Trajectory analysis.—For each system, all of the water molecules and Cl^- counterions are removed. The trajectories were combined and aligned together. Saved snapshots were analyzed using *cpptraj* module in AmberTools or UCSF Chimera. All graphics are produced using Pymol and UCSF Chimera.

Conclusion

In this work, we propose a new SIRT6 activation mechanism that depends on the proper interactions between NAD^+ and acetylated substrates, highlighting the importance of protein-cofactor-substrate interactions in the enzyme activation mechanism. We investigated the substrate selectivity of SIRT6 based on extensive molecular dynamic simulations and found that long-chain substrates can well occupy the hydrophobic pocket between the zinc-binding motif domain and the Rossmann folding domain; thus long-chain substrates can stabilize the catalytically favourable conformation of NAD^+. Inspired by this observation, we further proposed a rational binding mode for myristic acid and show that this endogenous SIRT6 activator facilitates the catalytic process by stabilizing the binding of NAD^+ and acetylated substrates. To verify the generality of our findings, we investigated three synthetic SIRT6 activator molecules, and the experimental results showed that they, as well as myristic acid, could restore the hydrogen bond of ribose to His131 to prevent the flipping of ribose, stabilizing the rational conformation of NAD^+ (Figure 5).

In our previous studies, we have reported the activation mechanism of SIRT1 and HDAC8.[33, 34] The interaction between the protein and substrate stabilized by natural products resveratrol in human SIRT1 activation and reinstate the tight binding of SIRT1 to specific “loosely bound” substrates. Similar to the activation mechanism of SIRT1, the activation of HDAC8 also depends on the stability of the interaction between HDAC8 and fluorescent substrate, resulting in favourable catalytic conformational changes. Along with SIRT1 and HDAC8, our proposed activation of SIRT6 further emphasized the importance of maintaining proper protein-substrate interactions in small molecule induced enzyme activation.

In summary, our study further elucidates the mechanism of activation of SIRT6 at the atomic level and proposes a strategy to approximate the catalytic activity of the protein by the dihedral angle distribution. These results will facilitate the design and optimization of novel SIRT6 activators.

Supplementary Material

Refer to Web version on PubMed Central for supplementary material.

ACKNOWLEDGMENTS

This work was supported by National Natural Science Foundation of China (82003590 and 92053105), Natural Science Foundation of Shandong Province (ZR2020QH342 and ZR2022QH209). Y.Z. would like to acknowledge the support of NIH (R35-GM127040).

Data availability statement

Data used to generate MD results including parameter files and topology files as well as MD trajectory files are available online at https://doi.org/10.17605/OSF.IO/VYR6Z.

Reference

1. Finkel T; Deng CX; Mostoslavsky R, Recent progress in the biology and physiology of sirtuins. Nature 2009, 460, 587–91. [PubMed: 19641587]
2. Xu Z; Zhang L; Zhang W; Meng D; Zhang H; Jiang Y; Xu X; Van Meter M; Seluanov A; Gorbunova V; Mao Z, SIRT6 rescues the age related decline in base excision repair in a PARP1-dependent manner. Cell Cycle 2015, 14, 269–76. [PubMed: 25607651]
3. Masri S., Sirtuin-dependent clock control: new advances in metabolism, aging and cancer. Curr Opin Clin Nutr Metab Care 2015, 18, 521–7. [PubMed: 26335311]
4. Wang ZA; Markert JW; Whedon SD; Yapa Abeywardana M; Lee K; Jiang H; Suarez C; Lin H; Farnung L; Cole PA, Structural Basis of Sirtuin 6-Catalyzed Nucleosome Deacetylation. J Am Chem Soc 2023, 145, 6811–6822. [PubMed: 36930461]

5. Chio US; Rechiche O; Bryll AR; Zhu J; Leith EM; Feldman JL; Peterson CL; Tan S; Armache J-P, Cryo-EM structure of the human Sirtuin 6–nucleosome complex. Sci Adv 2023, 9, eadf7586. [PubMed: 37058572]

6. Michishita E; McCord RA; Boxer LD; Barber MF; Hong T; Gozani O; Chua KF, Cell cycle-dependent deacetylation of telomeric histone H3 lysine K56 by human SIRT6. Cell Cycle 2009, 8, 2664–6. [PubMed: 19625767]

7. Etchegaray JP; Zhong L; Li C; Henriques T; Ablondi E; Nakadai T; Van Rechem C; Ferrer C; Ross KN; Choi JE; Samarakkody A; Ji F; Chang A; Sadreyev RI; Ramaswamy S; Nechaev S; Whetstine JR; Roeder RG; Adelman K; Goren A; Mostoslavsky R, The Histone Deacetylase SIRT6 Restrains Transcription Elongation via Promoter-Proximal Pausing. Mol Cell 2019, 75, 683–699 e7. [PubMed: 31399344]

8. Michishita E; McCord RA; Berber E; Kioi M; Padilla-Nash H; Damian M; Cheung P; Kusumoto R; Kawahara TL; Barrett JC; Chang HY; Bohr VA; Ried T; Gozani O; Chua KF, SIRT6 is a histone H3 lysine 9 deacetylase that modulates telomeric chromatin. Nature 2008, 452, 492–6. [PubMed: 18337721]

9. Bae EJ, Sirtuin 6, a possible therapeutic target for type 2 diabetes. Arch Pharm Res 2017, 40, 1380–1389. [PubMed: 29177584]

10. Klein MA; Denu JM, Biological and catalytic functions of sirtuin 6 as targets for small-molecule modulators. J Biol Chem 2020, 295, 11021–11041. [PubMed: 32518153]

11. Mautone N; Zwergel C; Mai A; Rotili D, Sirtuin modulators: where are we now? A review of patents from 2015 to 2019. Expert Opin Ther Pat 2020, 30, 389–407. [PubMed: 32228181]

12. Jiang H; Khan S; Wang Y; Charron G; He B; Sebastian C; Du J; Kim R; Ge E; Mostoslavsky R; Hang HC; Hao Q; Lin H, SIRT6 regulates TNF-alpha secretion through hydrolysis of long-chain fatty acyl lysine. Nature 2013, 496, 110–3. [PubMed: 23552949]

13. Feldman JL; Baeza J; Denu JM, Activation of the protein deacetylase SIRT6 by long-chain fatty acids and widespread deacylation by mammalian sirtuins. J Biol Chem 2013, 288, 31350–6. [PubMed: 24052263]

14. You W; Rotili D; Li TM; Kambach C; Meleshin M; Schutkowski M; Chua KF; Mai A; Steegborn C, Structural Basis of Sirtuin 6 Activation by Synthetic Small Molecules. Angew Chem Int Ed Engl 2017, 56, 1007–1011. [PubMed: 27990725]

15. Huang Z; Zhao J; Deng W; Chen Y; Shang J; Song K; Zhang L; Wang C; Lu S; Yang X; He B; Min J; Hu H; Tan M; Xu J; Zhang Q; Zhong J; Sun X; Mao Z; Lin H; Xiao M; Chin YE; Jiang H; Xu Y; Chen G; Zhang J, Identification of a cellularly active SIRT6 allosteric activator. Nat Chem Biol 2018, 14, 1118–1126. [PubMed: 30374165]

16. Chen X; Sun W; Huang S; Zhang H; Lin G; Li H; Qiao J; Li L; Yang S, Discovery of Potent Small-Molecule SIRT6 Activators: Structure-Activity Relationship and Anti-Pancreatic Ductal Adenocarcinoma Activity. J Med Chem 2020, 63, 10474–10495. [PubMed: 32787077]

17. Lu S; Chen Y; Wei J; Zhao M; Ni D; He X; Zhang J, Mechanism of allosteric activation of SIRT6 revealed by the action of rationally designed activators. Acta Pharm Sin B 2021, 11, 1355–1361. [PubMed: 34094839]

18. You W; Steegborn C, Structural Basis for Activation of Human Sirtuin 6 by Fluvastatin. ACS Med Chem Lett 2020, 11, 2285–2289. [PubMed: 33214841]

19. You W; Zheng W; Weiss S; Chua KF; Steegborn C, Structural basis for the activation and inhibition of Sirtuin 6 by quercetin and its derivatives. Sci Rep 2019, 9, 19176. [PubMed: 31844103]

20. Fiorentino F; Mai A; Rotili D, Emerging Therapeutic Potential of SIRT6 Modulators. J Med Chem 2021, 64, 9732–9758. [PubMed: 34213345]

21. Sacconnay L; Carrupt P-A; Nurisso A, Human sirtuins: Structures and flexibility. J Struct Biol 2016, 196, 534–542. [PubMed: 27773637]

22. Sanders BD; Jackson B; Marmorstein R, Structural basis for sirtuin function: What we know and what we don't. Biochim Biophys Acta Proteins Proteom 2010, 1804, 1604–1616.

23. Costantini S; Sharma A; Raucci R; Costantini M; Autiero I; Colonna G, Genealogy of an ancient protein family: the Sirtuins, a family of disordered members. BMC Evol Biol 2013, 13, 60. [PubMed: 23497088]

24. Pan PW; Feldman JL; Devries MK; Dong A; Edwards AM; Denu JM, Structure and biochemical functions of SIRT6. J Biol Chem 2011, 286, 14575–87. [PubMed: 21362626]
25. Shi Y; Zhou Y; Wang S; Zhang Y, Sirtuin Deacetylation Mechanism and Catalytic Role of the Dynamic Cofactor Binding Loop. J Phys Chem Lett 2013, 4, 491–495. [PubMed: 23585919]
26. Djokovic N; Ruzic D; Rahnasto-Rilla M; Srdic-Rajic T; Lahtela-Kakkonen M; Nikolic K, Expanding the Accessible Chemical Space of SIRT2 Inhibitors through Exploration of Binding Pocket Dynamics. J Chem Inf Model 2022, 62, 2571–2585. [PubMed: 35467856]
27. Singh M; Srivastava M; Wakode SR; Asthana S, Elucidation of Structural Determinants Delineates the Residues Playing Key Roles in Differential Dynamics and Selective Inhibition of Sirt1-3. J Chem Inf Model 2021, 61, 1105–1124. [PubMed: 33606530]
28. Muvva C; Murugan NA; Kumar Choutipalli VS; Subramanian V, Unraveling the Unbinding Pathways of Products Formed in Catalytic Reactions Involved in SIRT1–3: A Random Acceleration Molecular Dynamics Simulation Study. J Chem Inf Model 2019, 59, 4100–4115. [PubMed: 31553614]
29. Dolinsky TJ; Nielsen JE; McCammon JA; Baker NA, PDB2PQR: an automated pipeline for the setup of Poisson-Boltzmann electrostatics calculations. Nucleic Acids Res 2004, 32, W665–7. [PubMed: 15215472]
30. Dolinsky TJ; Czodrowski P; Li H; Nielsen JE; Jensen JH; Klebe G; Baker NA, PDB2PQR: expanding and upgrading automated preparation of biomolecular structures for molecular simulations. Nucleic Acids Res 2007, 35, W522–5. [PubMed: 17488841]
31. Peters MB; Yang Y; Wang B; Fusti-Molnar L; Weaver MN; Merz KM Jr., Structural Survey of Zinc Containing Proteins and the Development of the Zinc AMBER Force Field (ZAFF). J Chem Theory Comput 2010, 6, 2935–2947. [PubMed: 20856692]
32. Ryde U., On the role of Glu-68 in alcohol dehydrogenase. Protein Sci 1995, 4, 1124–32. [PubMed: 7549877]
33. Du J; Li W; Liu B; Zhang Y; Yu J; Hou X; Fang H, An in silico mechanistic insight into HDAC8 activation facilitates the discovery of new small-molecule activators. Bioorg Med Chem 2020, 28, 115607. [PubMed: 32690262]
34. Hou X; Rooklin D; Fang H; Zhang Y, Resveratrol serves as a protein-substrate interaction stabilizer in human SIRT1 activation. Sci Rep 2016, 6, 38186. [PubMed: 27901083]

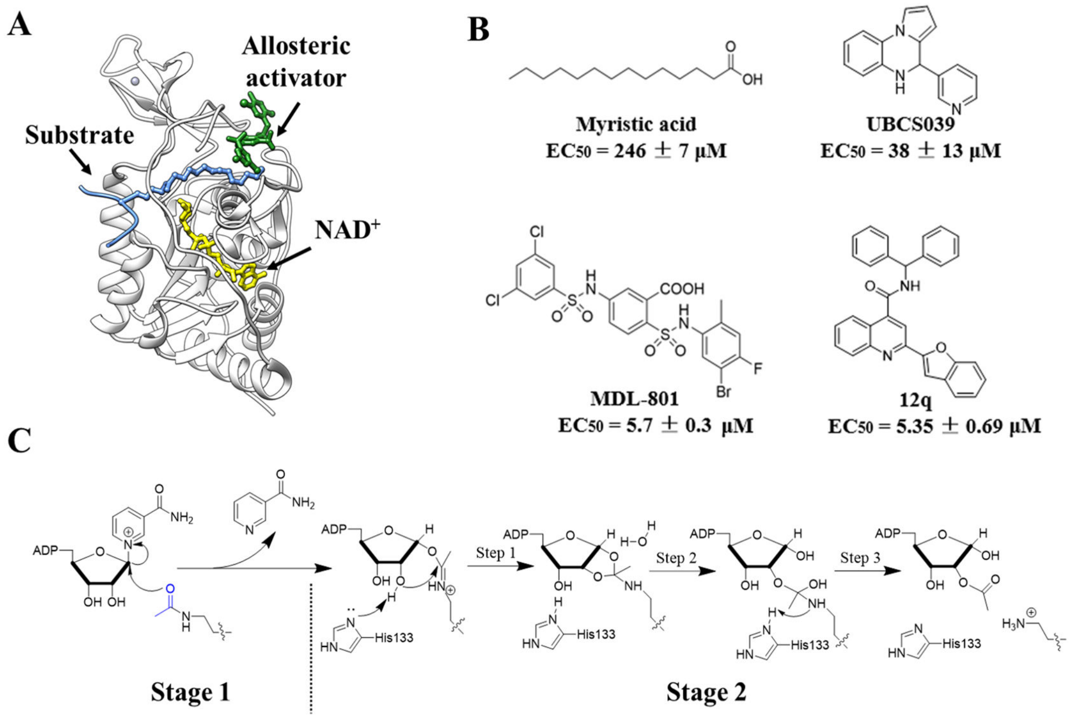

Figure 1.

The protein structure, small molecular activators and proposed catalytic mechanism of SIRT6. (A) Structures of SIRT6 with substrate and NAD^+ complex (PDB ID: 5Y2F). (B) Small molecular SIRT6 activators. (C) The proposed catalytic mechanism for deacetylation reaction of Sirtuin.

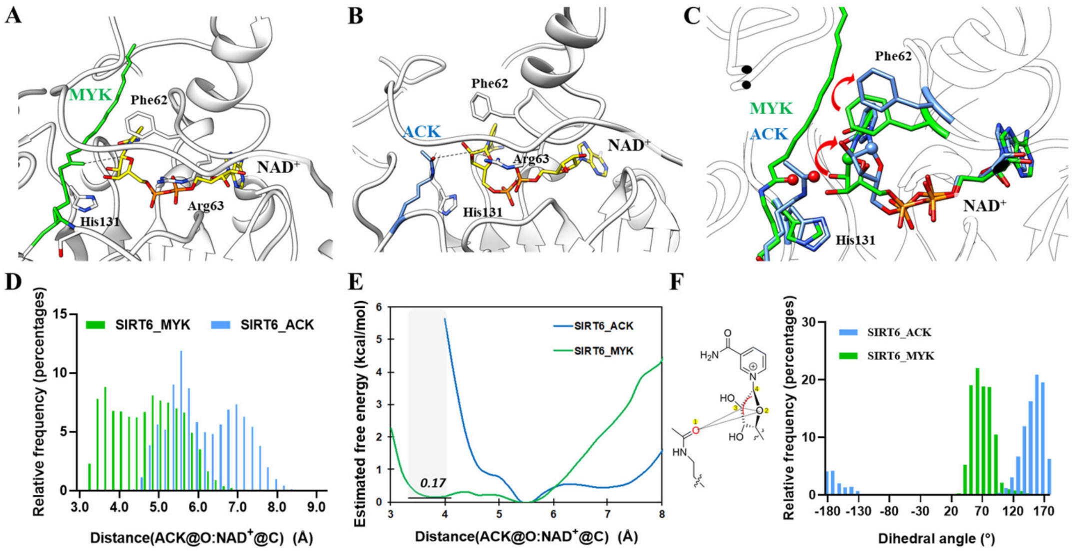

Figure 2.

Comparison of the binding of acetylated substrate and myristoylated substrate with SIRT6. (A) Representative structure of the SIRT6-NAD$^+$-Myristic substrate complex. (B) Representative structure of the SIRT6-NAD$^+$-Acetyl lysine substrate complex. (C) Comparison of the SIRT6-ACK complex and the SIRT6-MYK complex. (D) The distance distribution between ACK/MYK@O and NAD$^+$@C. (E) Estimated catalytic free energy values calculated on the ACK/MYK@O:NAD$^+$@C distance. (F) Diagram and distribution of the key dihedral angle between the substrate and cofactor, which is essential for the catalytic reaction. The four atoms that make up the dihedral angle are marked by yellow dots.

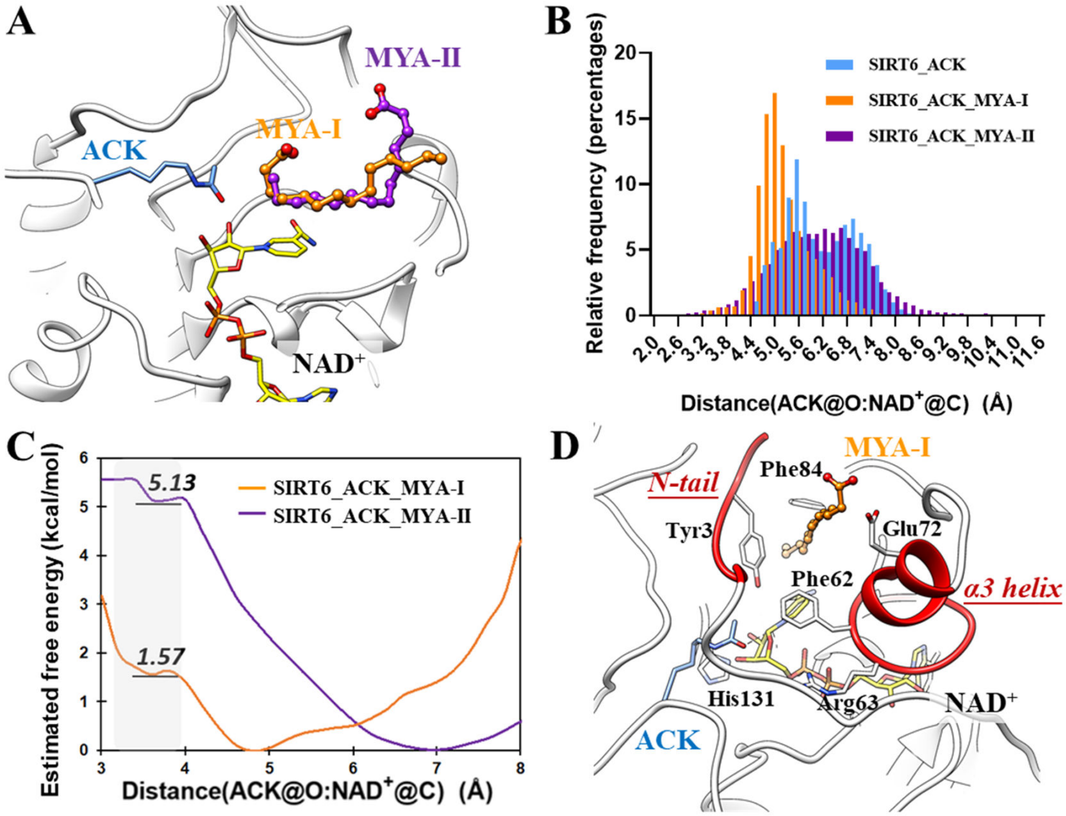

Figure 3.

The precited binding mode of myristic acid with SIRT6. (A) Initial docking poses for MYA-I and MYA-II. (B) The distance distribution between ACK@O and NAD$^+$@C. (C) The estimated catalytic free energy values are calculated on ACK@O: NAD$^+$@C distance. (D) The representative binding mode of MYA-I after MD simulation. The NAD$^+$ is shown as yellow sticks, peptide substrate is shown in blue, and myristic acid is shown as orange sticks.

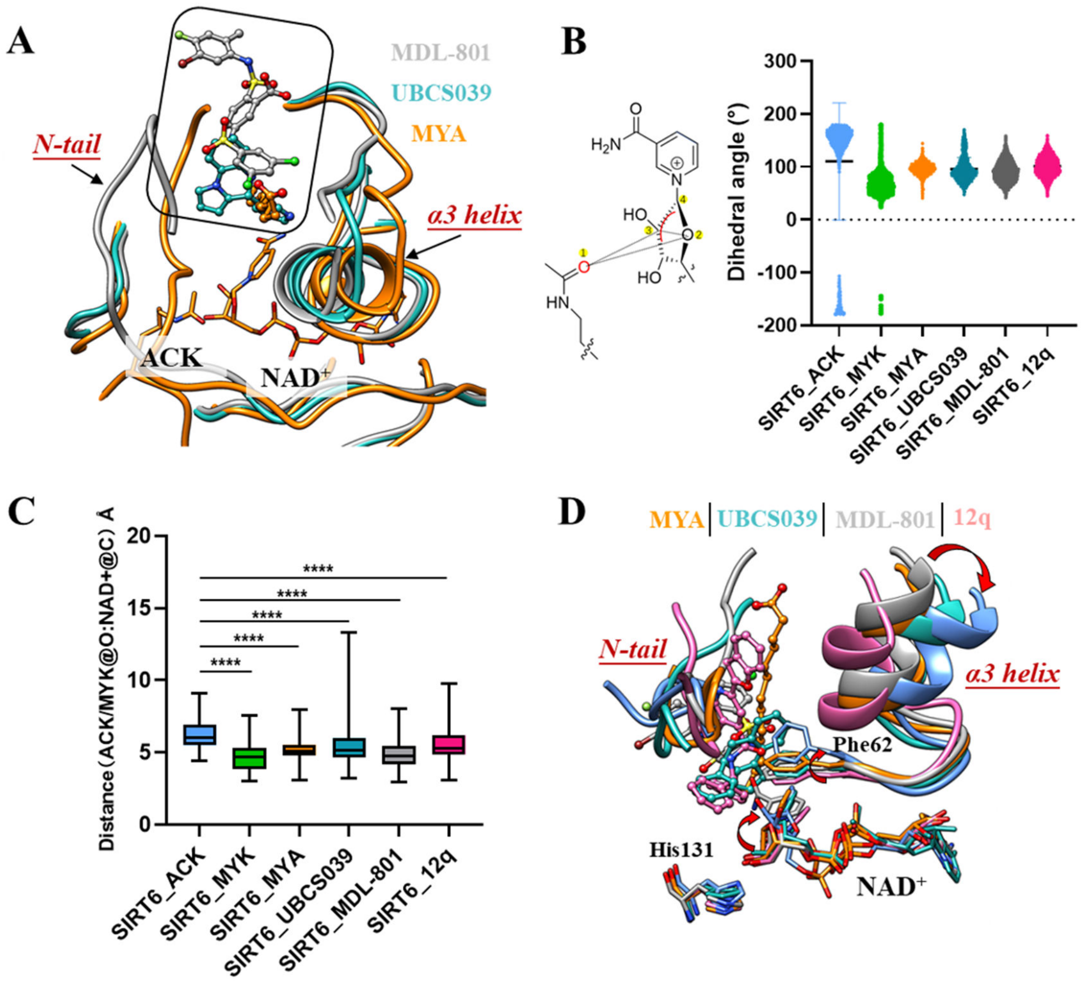

Figure 4.

Comparison of the binding of different small molecular activators with SIRT6. (A) Comparison of predicted binding pose of MYA-I and known SIRT6 activators MDL-801 and UBCS039 from crystal structures. (B) Distribution of the key dihedral angle between the substrate and the cofactor in different systems, which is essential for the catalytic reaction. The four atoms that make up the dihedral angle are marked by yellow dots. (C) The distance distribution between ACK@O and NAD^+@C in different MD systems. (D) Comparison of the representative binding poses of different SIRT6 activators in MD simulation.

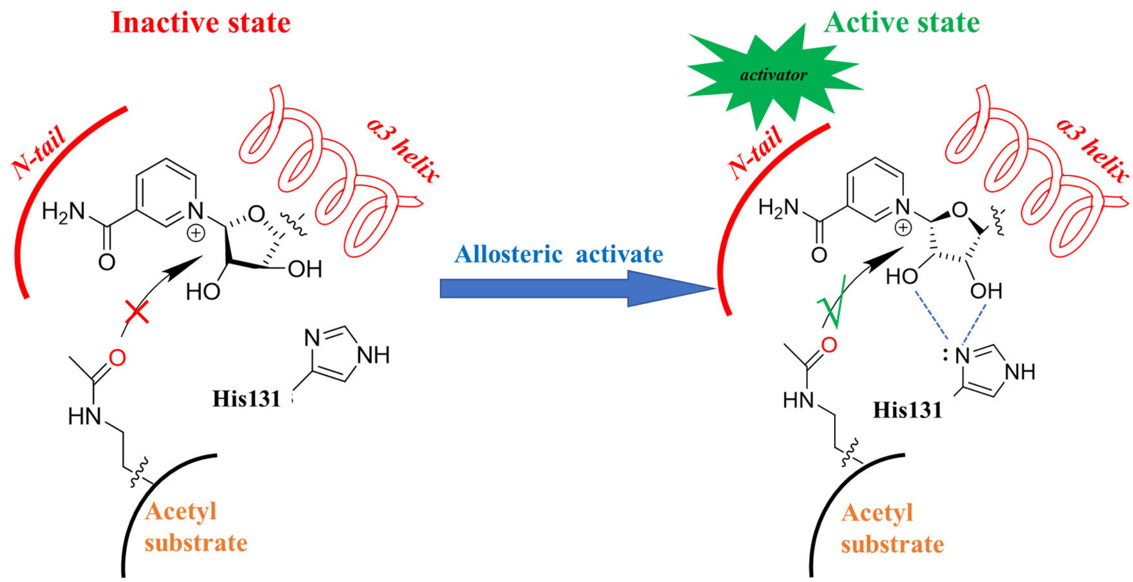

Figure 5.
The proposed allosteric activation mechanism of SIRT6.

Table 1.

The protein-substrate complex systems used for MD simulations.

System	Substrate	Co-factor	Activator	MD time	Substrate binding
1	Acetyl-lysine (ACK)	NAD^+	-	2 μs	Loose
2	Myristoyl-lysine (MYK)	NAD^+	-	2 μs	Tight
3	Acetyl-lysine (ACK)	NAD^+	Myristic acid (MYA-I)	2 μs	Tight
4	Acetyl-lysine (ACK)	NAD^+	Myristic acid (MYA-II)	2 μs	Loose
5	Acetyl-lysine (ACK)	NAD^+	MDL-801	2 μs	Tight
6	Acetyl-lysine (ACK)	NAD^+	12q	2 μs	Tight
7	Acetyl-lysine (ACK)	NAD^+	UBCS039	2 μs	Tight